Study of pentaquark systems

Author: Yuri Sánchez Alves
*Facultat de Física, Universitat de Barcelona, Diagonal 645, 08028 Barcelona, Catalonia, Spain.**

Advisor: Àngels Ramos Gómez

Abstract: In this work we study the possible existence of pentaquarks in the hidden charm sector that could be interpreted as meson-baryon molecular states. Employing a vector-meson exchange mechanism for the interaction between mesons and baryons we obtain molecular-type pentaquark resonances for the lowest isospin configuration in each strangeness sector and compare them to experimental findings.

I. INTRODUCTION

From the beginning of the millennium many exotic multiquark hadrons have been observed experimentally. These states have more complex structures than those of the conventional quark model, which essentially describes mesons as quark-antiquark pairs and baryons as three quarks. In particular, the study of pentaquark baryons is an active field of research. In 2015 the LHCb collaboration discovered two pentaquark states in the $J/\psi\, p$ mass spectrum of the $\Lambda_b^0 \to J/\psi\, K^- p$ decay [1]. These two states were denoted as $P_c(4380)^+$ and $P_c(4450)^+$. However, later, in 2019, these discoveries were reexamined by the same LHCb collaboration. The experiments showed the existence of a state at lower energy, $P_c(4312)^+$, and the 4450 peak was found to be composed of two different states, $P_c(4440)^+$ and $P_c(4457)^+$, while the existence of the $P_c(4380)^+$ was put in doubt [2]. The quantum numbers of such states were compatible with those of a nucleon resonance, which is understood in the conventional quark model as composed by three quarks of u and d flavour. However, the high mass of the found states inevitably demands the presence of an additional $c\bar{c}$ pair, thus providing clear evidence for the existence of pentaquarks in the strangeness $S = 0$ sector. In the case of strangeness $S = -1$, the LHCb collaboration found evidence for two states, $P_{cs}(4459)^+$ [3] and $P_{cs}(4338)^+$ [4]. For strangeness $S = -2$ no such states have been found yet. This is the current experimental situation of pentaquark states. In this work we perform a theoretical study of hidden charm ($c\bar{c}$) pentaquark states with strangeness $S = 0, -1, -2$ which can be interpreted as bound meson-baryon pairs, also known as meson-baryon molecules. The molecular picture has gained interest recently due to the proximity of the observed exotic states to various meson-baryon energy thresholds. To fulfill the purpose of our research, we adopt a model for the interaction between mesons and baryons which is based on a vector meson exchange mechanism. This model has already been discussed in previous articles with promising results [5–10].

*Electronic address: ysanalves6@gmail.com

II. FORMALISM

The model employed in this work relies on a meson-baryon interaction in s-wave, which is built up from the t-channel vector-meson exchange diagram of Fig. 1, where the mesons are depicted by dashed lines and the baryons by solid lines. The external mesons in the diagram represent the ground states of either pseudoscalar ($J^P(M) = 0^-$) or vector ($J^P(M) = 1^-$)-type, while the baryons are the lowest-energy ones with $J^P(B) = 1/2^+$, all of them composed out of u, d, s, c quarks and, in the case of mesons, their corresponding antiquarks. The indices i, j label the different meson-baryon channels with the same spin-parity (J^P), isospin and flavour quantum numbers that can be connected by the exchange of a vector meson V^*. The vertices in that diagram are obtained from the local hidden vector meson formalism [5] via the following Lagrangians

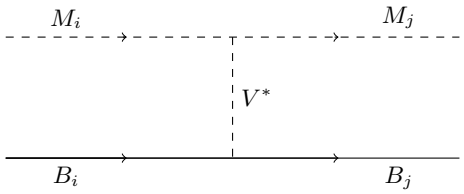

FIG. 1: Meson-Baryon interaction tree level diagram.

$$\mathcal{L}_{VPP} = ig\langle[\partial_\mu\phi, \phi]\, V^\mu\rangle, \tag{1}$$

$$\mathcal{L}_{VBB} = \frac{g}{2}\sum_{i,j,k,l=1}^{4} \bar{B}_{ijk}\gamma^\mu \left(V^k_{\mu,l}B^{ijl} + 2V^j_{\mu,l}B^{ilk}\right), \tag{2}$$

$$\mathcal{L}_{VVV} = ig\langle[V^\mu, \partial_\nu V_\mu]\, V^\nu\rangle, \tag{3}$$

where the symbol $\langle\ \rangle$ denotes the trace of $SU(4)$ matrices in flavour space, and the factor g is the universal coupling constant, related to the pion decay constant $f = 93$ MeV by $g = m_V/2f$ with m_V being a representative mass of the light (uncharmed) vector mesons from the nonet. Using the above vertices one obtains the t-channel Vector-

Meson-Exchange (TVME) potential [5]:

$$V_{ij} = g^2 \sum_v C_{ij}^v \bar{u}(p_j)\gamma^\mu u(p_i) \frac{1}{t-m_v^2} \times \left[(k_i+k_j)_\mu - \frac{k_i^2-k_j^2}{m_v^2}(k_i-k_j)_\mu \right], \quad (4)$$

where p_i, p_j (k_i, k_j) are the four-momenta of the baryons (mesons) in the i, j channels and m_v is the mass of the vector meson exchanged. Adopting the same mass $m_v = m_V$ for the light vector mesons and accounting for the higher mass of the charmed mesons with a common multiplying factor $\kappa_c = (m_V/m_V^c)^2 \approx 1/4$ and for the $c\bar{c}$ mesons with $\kappa_{cc} = (m_V/m_V^{cc})^2 \approx 1/9$, Eq. (4) simplifies to

$$V_{ij} = -C_{ij}\frac{1}{4f^2}\bar{u}(p_j)\gamma^\mu u(p_i)(k_i+k_j)_\mu , \quad (5)$$

where the limit $t \ll m_V$ has been taken to reduce the t-channel diagram to a contact term. The coefficients C_{ij} are symmetric with respect to the indices and are obtained summing the various vector meson exchange contributions, $\sum_v C_{ij}^v$, including the factor κ_c in the case of charmed mesons and κ_{cc} in the case of doubly charmed mesons. Developing the algebra up to order $\mathcal{O}(p^2/M^2)$, one reaches the expression:

$$V_{ij}(\sqrt{s}) = -C_{ij}\frac{1}{4f^2}\left(2\sqrt{s} - M_i - M_j\right) N_i N_j \quad (6)$$

where M_i, M_j and E_i, E_j are the masses and the energies of the baryons and $N = \sqrt{(E+M)/2M}$. Note that, while $SU(4)$ symmetry is encoded in the values of the coefficients C_{ij}^v, the interaction potential is not SU(4) symmetric due to the use of physical masses for the mesons and baryons involved, as well as to the factors κ_c and κ_{cc}.

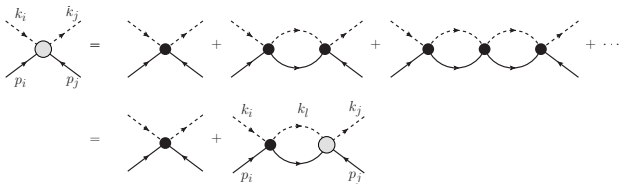

FIG. 2: Diagrams representing the Bethe-Salpeter equations in meson-baryon scattering. The big empty circle corresponds to the T_{ij} matrix element, the black circles correspond to the potential V_{ij} and the loops represent the propagator G_l function. The i, j, l indices stand for the channels of the coupled-channels.

The scattering amplitude T_{ij} is unitarized via the coupled-channel Bethe-Salpeter (B-S) equation, which implements the resummation of loop diagrams to infinite order schematically depicted in Fig. 2 and has the expression

$$T_{ij} = V_{ij} + V_{il}G_l T_{lj}. \quad (7)$$

Factorizing the V and T matrices on-shell out of the internal integrals implicit in Eq. (7) its solution,

$$T = (1 - VG)^{-1}V , \quad (8)$$

is purely algebraic. The mass (M) and width (Γ) of the sought resonances are obtained from the scattering amplitude in the complex plane. In the neighbourhood of a pole, this scattering amplitude, behaves as

$$T_{ij} \sim \frac{g_i\, g_j}{z - z_{pole}} \quad (9)$$

where $z_{pole} = M + i\Gamma/2$ and g_i are the coupling constants of the resonance to the different channels.

The loop function is given by

$$G_l = i\int \frac{d^4q}{(2\pi)^4}\frac{2M_l}{(P-q)^2 - M_l^2 + i\epsilon}\frac{1}{q^2 - m_l^2 + i\epsilon}, \quad (10)$$

where M_l and E_l correspond to the mass and the energy of the intermediate baryon, m_l is the mass of the intermediate meson, $P = k + p = (\sqrt{s}, \vec{0})$ is the total four-momentum of the system in the centre of mass (cm) frame and q denotes the four-momentum of the meson propagating in the intermediate loop. This function diverges logarithmically and so must be properly regularized. One may employ the *cut-off* regularization method, which consists in replacing the infinite upper limit of the integral by a large enough cut-off momentum Λ,

$$G_l^{\rm cut} = \int_0^\Lambda \frac{d^3q}{(2\pi)^3}\frac{1}{2\omega_l(\vec{q})}\frac{M_l}{E_l(\vec{q})}\frac{1}{\sqrt{s} - \omega_l(\vec{q}) - E_l(\vec{q}) + i\epsilon}, \quad (11)$$

or the alternative *dimensional regularization* (DR) approach, which is the one adopted here:

$$\begin{aligned} G_l = \frac{2M_l}{16\pi^2}\Big\{ & a_l(\mu) + \ln\frac{M_l^2}{\mu^2} + \frac{m_l^2 - M_l^2 + s}{2s}\ln\frac{m_l^2}{M_l^2} + \\ & + \frac{q_l}{\sqrt{s}}\Big[\ln\left(s - (M_l^2 - m_l^2) + 2q_l\sqrt{s}\right) \\ & + \ln\left(s + (M_l^2 - m_l^2) + 2q_l\sqrt{s}\right) \\ & - \ln\left(-s + (M_l^2 - m_l^2) + 2q_l\sqrt{s}\right) \\ & - \ln\left(-s - (M_l^2 - m_l^2) + 2q_l\sqrt{s}\right)\Big]\Big\}, \end{aligned} \quad (12)$$

where $a_l(\mu)$ is the subtraction constant at the regularization scale μ, and q_l is the on-shell three-momentum of the meson in the loop. The choice of the regularization scale μ and the corresponding subtraction constants $a_l(\mu)$ can be obtained by demanding that, at an energy close to the channel threshold, G_l is similar to $G_l^{\rm cut}$ for a certain cut-off Λ, namely

$$a_l(\mu) = \frac{16\pi^2}{2M_l}\left(G_l^{\rm cut}(\Lambda) - G_l(\mu, a_l = 0)\right). \quad (13)$$

The value of Λ here is taken to be 800 MeV as it is close to the masses of the light vector mesons exchanged, which

are integrated out when reducing the t-channel contribution to a contact interaction. The lighter of these is the vector meson $\rho(770)$ so the cut-off we use is a reasonable choice [8].

In Tables I to III we present the scattering coefficients C_{ij} in Eq. (6) obtained for each strangeness sector in the case of the interaction of pseudoscalar mesons with baryons (from now on denoted as PB interaction). Only the heavy channels have been kept since they have been found to essentially decouple from the light ones. The corresponding coefficients for the interaction of vector mesons with baryons (from now on denoted as VB interaction) are exactly the same as those in Tables I to III, requiring only the substitutions: $\bar{D} \to \bar{D}^*$, $\eta_c \to J/\psi$, $\bar{D}_s \to \bar{D}_s^*$

	$\eta_c N$	$\bar{D}\Lambda_c$	$\bar{D}\Sigma_c$
$\eta_c N$	0	$-\sqrt{\frac{3}{2}}\kappa_c$	$\sqrt{\frac{3}{2}}\kappa_c$
$\bar{D}\Lambda_c$		$-1+\kappa_{cc}$	0
$\bar{D}\Sigma_c$			$1+\kappa_{cc}$

TABLE I: C_{ij} coefficients in the $(I,S)=(\frac{1}{2},0)$ sector

	$\eta_c\Lambda$	$\bar{D}_s\Lambda_c$	$\bar{D}\Xi_c$	$\bar{D}\Xi_c'$
$\eta_c\Lambda$	0	κ_c	$-\frac{1}{\sqrt{2}}\kappa_c$	$-\sqrt{\frac{3}{2}}\kappa_c$
$\bar{D}_s\Lambda_c$		κ_{cc}	$\sqrt{2}$	0
$\bar{D}\Xi_c$			$1+\kappa_{cc}$	0
$\bar{D}\Xi_c'$				$1+\kappa_{cc}$

TABLE II: C_{ij} coefficients in the $(I,S)=(0,-1)$ sector

	$\eta_c\Xi$	$\bar{D}_s\Xi_c$	$\bar{D}_s\Xi_c'$	$\bar{D}\Omega_c$
$\eta_c\Xi$	0	$\sqrt{\frac{3}{2}}\kappa_c$	$\frac{1}{\sqrt{2}}\kappa_c$	$-\kappa_c$
$\bar{D}_s\Xi_c$		$-1+\kappa_{cc}$	0	0
$\bar{D}_s\Xi_c'$			$-1+\kappa_{cc}$	$-\sqrt{2}$
$\bar{D}\Omega_c$				κ_{cc}

TABLE III: C_{ij} coefficients in the $(I,S)=(\frac{1}{2},-2)$ sector

III. RESULTS AND DISCUSSION

In this section we present an ordered list of the results we have obtained. First of all, using a cut-off of Λ=800 MeV we found the values of the subtraction constants for the heavy channels displayed in Tables IV and V .

With the subtraction constants of Tables IV and V, we can obtain the loop functions employing Eq. (12) and the corresponding coupled-channel scattering amplitude T in

$(\frac{1}{2},0)$	$a_{\eta_c N}$	$a_{\bar{D}\Lambda_c}$	$a_{\bar{D}\Sigma_c}$	
	-2.40	-2.22	-2.28	
$(0,-1)$	$a_{\eta_c\Lambda}$	$a_{\bar{D}_s\Lambda_c}$	$a_{\bar{D}\Xi_c}$	$a_{\bar{D}\Xi_c'}$
	-2.40	-2.25	-2.29	-2.33
$(\frac{1}{2},-2)$	$a_{\eta_c\Xi}$	$a_{\bar{D}_s\Xi_c}$	$a_{\bar{D}_s\Xi_c'}$	$a_{\bar{D}\Omega_c}$
	-2.40	-2.31	-2.35	-2.37

TABLE IV: Values of the subtraction constants for the heavy channels in each (I,S) sector at a regularization scale $\mu=1$ GeV for the PB interaction .

$(\frac{1}{2},0)$	$a_{J/\psi}$	$a_{\bar{D}^*\Lambda_c}$	$a_{\bar{D}^*\Sigma_c}$	
	-2.46	-2.26	-2.32	
$(0,-1)$	$a_{J/\psi\Lambda}$	$a_{\bar{D}_s^*\Lambda_c}$	$a_{\bar{D}^*\Xi_c}$	$a_{\bar{D}^*\Xi_c'}$
	-2.45	-2.29	-2.32	-2.36
$(\frac{1}{2},-2)$	$a_{J/\psi\Xi}$	$a_{\bar{D}_s^*\Xi_c}$	$a_{\bar{D}_s^*\Xi_c'}$	$a_{\bar{D}\Omega_c}$
	-2.45	-2.35	-2.38	-2.40

TABLE V: Values of the subtraction constants for the heavy channels in each (I,S) sector at a regularization scale $\mu=1$ GeV for the VB interaction.

each (I,S) sector from Eq. (8). This amplitude is a complex matrix that may have poles, which correspond to the molecular-states we are seeking. These poles are found using a computer program which employs the steepest descent method. Furthermore, we can use the associated residues to obtain the coupling of the pole to each channel, according to Eq. (9). The results are shown in Tables VI and VII for the PB and VB interaction, respectively. Note that the PB states have spin-parity $J^p=\frac{1}{2}^-$ since they are obtained from an interaction of a pseudoscalar (0^-) meson with a $\frac{1}{2}^+$ baryon in s-wave. However, the VB states can have either $J^p=\frac{1}{2}^-$ or $\frac{3}{2}^-$ since they are obtained from the s-wave interaction of a vector-meson (1^-) with a $\frac{1}{2}^+$ baryon.

Upon inspecting Tables VI and VII we observe that we obtain molecular meson-baryon states in each of the sectors considered. More specifically, in the PB case, we obtain a pentaquark with strangeness 0 that couples strongly to $\bar{D}\Sigma_c$, two pentaquarks with strangeness -1, one coupling strongly to $\bar{D}\Xi_c$ and the other to $\bar{D}\Xi_c'$, and finally a pentaquark with strangeness -2 that couples strongly to $\bar{D}\Omega_c$. We find an equivalent structure in the case of the VB interaction, with the difference that the pentaquarks appear at around 150 MeV higher in energy (which is the mass difference between pseudoscalar and vector mesons). The other difference is that the VB states are degenerate in spin-parity as they can have

(I,S)			g_a	
z_{pole} (MeV)				
$(\frac{1}{2},0)$	$\eta_c N$	$\bar{D}\Lambda_c$	$\bar{D}\Sigma_c$	
	(3919)	(4152)	(4319)	
4257.86+19.29i	1.29	0.23	3.04	
$(0,1)$	$\eta_c\Lambda$	$\bar{D}_s\Lambda_c$	$\bar{D}\Xi_c$	$\bar{D}\Xi_c'$
	(4095)	(4253)	(4336)	(4444)
4215.42+1.11i	0.34	1.49	3.06	0.14
4381.19+19.88i	1.16	0.19	0.15	3.01
$(\frac{1}{2},-2)$	$\eta_c\Xi$	$\bar{D}_s\Xi_c$	$\bar{D}_s\Xi_c'$	$\bar{D}\Omega_c$
	(4298)	(4438)	(4545)	(4564)
4493.54+18.04i	1.11	0.24	1.57	2.58

TABLE VI: Pole positions z_{pole} and coupling constants g_a for the $\frac{1}{2}^-$ states from PB $\rightarrow$ PB. Below each channel, the threshold energy in MeV is written between parenthesis.

(I,S)			g_a	
z_{pole} (MeV)				
$(\frac{1}{2},0)$	$J/\Psi N$	$\bar{D}^*\Lambda_c$	$\bar{D}^*\Sigma_c$	
	(4032)	(4293)	(4461)	
4398.97+19.15i	1.19	0.24	3.06	
$(0,-1)$	$J/\Psi\Lambda$	$\bar{D}_s^*\Lambda_c$	$\bar{D}^*\Xi_c$	$\bar{D}^*\Xi_c'$
	(4213)	(4397)	(4478)	(4585)
4359.72+1.24i	0.35	1.47	3.08	0.15
4522.52+19.80i	1.15	0.19	0.16	3.03
$(\frac{1}{2},-2)$	$J/\Psi\Xi$	$\bar{D}_s^*\Xi_c$	$\bar{D}_s^*\Xi_c'$	$\bar{D}^*\Omega_c$
	(4415)	(4581)	(4689)	(4706)
4635.91+18.34i	1.10	0.25	1.59	2.58

TABLE VII: Pole positions z_{pole} and coupling constants g_a for the $\frac{1}{2}^-$, $\frac{3}{2}^-$ states from VB $\rightarrow$ VB. Below each channel, the threshold energy in MeV is written between parenthesis.

$J^p = \frac{1}{2}^-$ and $J^p = \frac{3}{2}^-$. We would now like to represent graphically how these states could be seen in an experiment. For this reason, we represent in Fig. 3 the quantity $q_{cm}^j \cdot |T_{ij}|^2$ as a function of the center of mass energy $\sqrt{s}$, for each sector. In the above expression, the index i labels the channel to which the resonance couples most, and the index j represents the channel in which the resonance can decay with higher probability. The quantity q_{cm}^j stands for the center of mass (cm) momentum in the final state and acts as a phase-space modulator.

The PB states are depicted by blue lines and the VB ones by red lines. For $S = 0$ we observe a peak corresponding to the transition $\bar{D}\Sigma_c \rightarrow \eta_c N$ in the PB case and $\bar{D}^*\Sigma \rightarrow J/\psi N$ in the VB case. For $S = -1$ we find two peaks for each type of interaction. The first peak (solid lines) corresponds to the $\bar{D}\Xi_c \rightarrow \eta_c\Lambda$ transition for the PB case and the $\bar{D}^*\Xi_c \rightarrow J/\psi\Lambda$ transition for the VB case. The second peak (dashed lines) corresponds to the $\bar{D}\Xi_c' \rightarrow \eta_c\Lambda$ transition in the PB case and to the

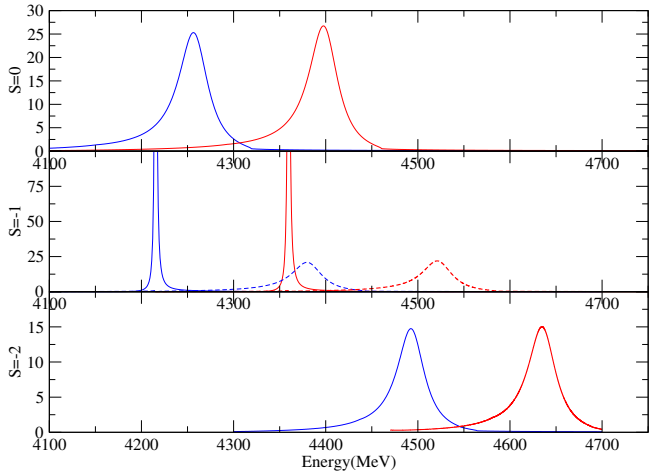

FIG. 3: Representation of $q_{cm}^j \cdot |T_{ij}|^2$ as a function of the cm energy for the i, j channels with the strongest coupling to the resonance.

$\bar{D}^*\Xi_c' \rightarrow J/\psi\Lambda$ transition in the VB case. For $S = -2$ we observe a peak corresponding to the $\bar{D}\Omega_c \rightarrow \eta_c\Xi$ transition in the PB case and to the $\bar{D}^*\Omega_c \rightarrow J/\psi\Xi$ transition in the VB case. Finally, in Figures 4 to 6 we compare the energy and width of our PB and VB pentaquark candidates (using the same colour code as in Fig. 3) with the experimental states. Notice that all but one experimental point are coloured in black. The gray colour is used instead of black to indicate the weak experimental evidence for the $P_c(4380)^+$ state [2]. Error bars are represented in its usual way. The dark rectangle bar represents the minimum width while the more transparent rectangle represents the maximum width according to the error of the width.

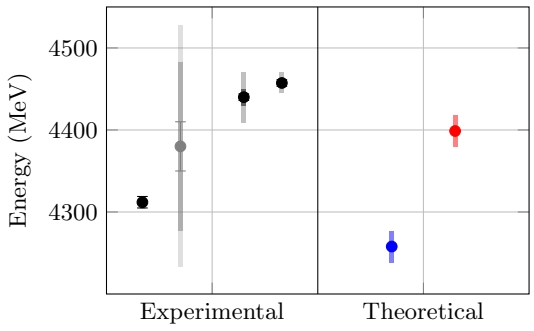

FIG. 4: This graphic represents both the experimental [2] and theoretical states for $S = 0$.

Comparing the experimental states in the $S = 0$ sector with our theoretical candidates, we find that the $P_c(4312)^+$ and $P_c(4440)^+$ states compare a bit above our predictions. It is interesting to point out that the poles would appear at higher energies by using a lower cut-off Λ. This is due to the fact that a lower cut-off limits the phase-space of the intermediate states, which translates into a lower binding energy. Now, we com-

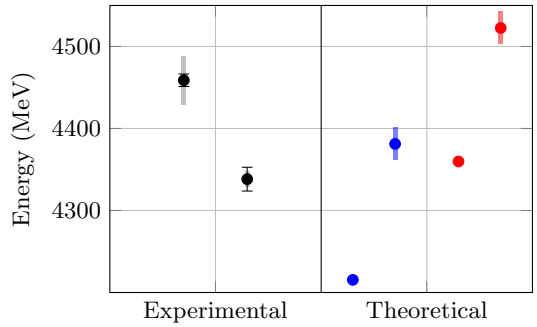

FIG. 5: This graphic represents both the experimental [3] [4] and theoretical states for $S = -1$.

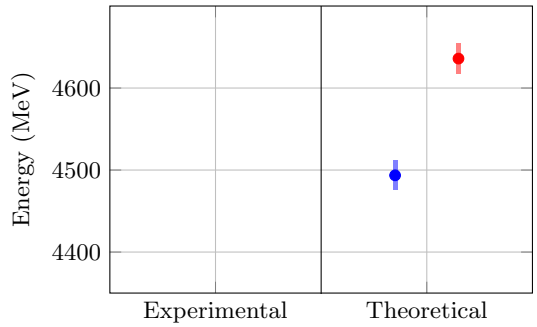

FIG. 6: This graphic represents the theoretical states for $S = -2$. To this day no such experimental states with $S = -2$ have been found.

pare the experimental states in the $S = -1$ sector with our theoretical candidates. The $P_{cs}(4459)^+$ state suits best the VB state we found at 4522 MeV. In a previous work [9] the proposed candidate for the $P_{cs}(4338)$ state was the VB state we found at 4359 MeV. However we would like to point out the possible correspondence of the experimental $P_{cs}(4338)$ to the PB candidate we found at 4381 MeV. Regarding the $S = -2$ sector, there are no experimental findings to this date. In this work we present possible candidates in this sector, at 4493.54 MeV and 4635.91 MeV, which compare very well with the theoretical candidates $P_{css}(4493)$ and $P_{css}(4633)$ found in [10] employing the cut-off regularization scheme.

IV. CONCLUSIONS

In this work, we have studied the possible existence of hidden charm pentaquarks employing a formalism that predicts them to be bound states of a meson and a baryon, commonly known as meson-baryon molecules. We have found several states in the various strangeness sectors and compared them to experimental data. After reviewing the results it is clear that our theoretical model gives molecular-type pentaquark candidates relatively close to the experimental states. By changing some factors, like the cut-off limit Λ or the coupling strength f, one could achieve slightly different results that could compare better to the experimental observations. This means that our theory offers a good explanation for the observed states, although more research needs to be carried out. Finally, since our model predicts some states that have not yet been found experimentally, our results should encourage experimental research that may shine a light on the nature of these pentaquark structures. In conclusion, the next few years will be of great relevance to clarify the validity of the model employed in this work, especially if the proposed theoretical candidates are found in the experiments.

Acknowledgments

First of all, I would like to express my gratitude to my advisor Dr Àngels Ramos for being so patient and dedicating many hours to this project. Not only has she been an incredible professor with her explanations but also an amazing guide in the endeavour of writing this paper. I would also like to thank my relatives and close ones for the support and encouragement.

[1] R. Aaij *et al.* [LHCb], Phys. Rev. Lett. **115**, 072001 (2015) doi:10.1103/PhysRevLett.115.072001 [arXiv:1507.03414 [hep-ex]].
[2] R. Aaij *et al.* [LHCb], Phys. Rev. Lett. **122**, no.22, 222001 (2019) doi:10.1103/PhysRevLett.122.222001 [arXiv:1904.03947 [hep-ex]].
[3] R. Aaij *et al.* [LHCb], Sci. Bull. **66**, 1278-1287 (2021) doi:10.1016/j.scib.2021.02.030 [arXiv:2012.10380 [hep-ex]].
[4] [LHCb], [arXiv:2210.10346 [hep-ex]].
[5] J. Hofmann and M. F. M. Lutz, Nucl. Phys. A **763**, 90-139 (2005) doi:10.1016/j.nuclphysa.2005.08.022 [arXiv:hep-ph/0507071 [hep-ph]].
[6] J. J. Wu, R. Molina, E. Oset and B. S. Zou, Phys. Rev. Lett. **105**, 232001 (2010) [arXiv:1007.0573 [nucl-th]].
[7] J. J. Wu, R. Molina, E. Oset and B. S. Zou, Phys. Rev. C **84**, 015202 (2011) doi:10.1103/PhysRevC.84.015202 [arXiv:1011.2399 [nucl-th]].
[8] G. Montaña, A. Feijoo and À. Ramos, Eur. Phys. J. A **54**, no.4, 64 (2018) doi:10.1140/epja/i2018-12498-1 [arXiv:1709.08737 [hep-ph]].
[9] A. Feijoo, W. F. Wang, C. W. Xiao, J. J. Wu, E. Oset, J. Nieves and B. S. Zou, Phys. Lett. B **839**, 137760 (2023) doi:10.1016/j.physletb.2023.137760 [arXiv:2212.12223 [hep-ph]].
[10] J.A.Marsé-Valera, V. K. Magas and A. Ramos, Phys. Rev. Lett. **130**, no.9, 9 (2023) doi:10.1103/PhysRevLett.130.091903 [arXiv:2210.02792 [hep-ph]].